Atmos. Chem. Phys., 14, 8255–8267, 2014
www.atmos-chem-phys.net/14/8255/2014/
doi:10.5194/acp-14-8255-2014

Atmospheric Chemistry and Physics Open Access

Contribution of ship traffic to aerosol particle concentrations downwind of a major shipping lane

N. Kivekäs[1,2], A. Massling[3], H. Grythe[2,4,5], R. Lange[6], V. Rusnak[1], S. Carreno[1], H. Skov[3,7,8], E. Swietlicki[1], Q. T. Nguyen[6], M. Glasius[6], and A. Kristensson[1]

[1]Department of Physics, Lund University, Lund, Sweden
[2]Atmospheric Composition, Finnish Meteorological Institute, Helsinki, Finland
[3]Department of Environmental Science, Aarhus University, Roskilde, Denmark
[4]Department of Applied Environmental Science, Stockholm University, Stockholm, Sweden
[5]Norwegian Institute for Air Research, Oslo, Norway
[6]Department of Chemistry and iNANO, Aarhus University, Aarhus, Denmark
[7]Arctic Research Centre, Aarhus University, Aarhus, Denmark
[8]University of Southern Denmark, Institute of Chemical Engineering and Biotechnology and Environmental Technology, Odense, Denmark

Correspondence to: N. Kivekäs (niku.kivekas@fmi.fi)

Received: 21 December 2013 – Published in Atmos. Chem. Phys. Discuss.: 31 March 2014
Revised: 24 June 2014 – Accepted: 13 July 2014 – Published: 19 August 2014

Abstract. Particles in the atmosphere are of concern due to their toxic properties and effects on climate. In coastal areas, ship emissions can be a significant anthropogenic source. In this study we investigated the contribution from ship emissions to the total particle number and mass concentrations at a remote location. We studied the particle number concentration (12 to 490 nm in diameter), the mass concentration (12 to 150 nm in diameter) and number and volume size distribution of aerosol particles in ship plumes for a period of 4.5 months at Høvsøre, a coastal site on the western coast of Jutland in Denmark. During episodes of western winds, the site is about 50 km downwind of a major shipping lane and the plumes are approximately 1 hour old when they arrive at the site. We have used a sliding percentile-based method for separating the plumes from the measured background values and to calculate the ship plume contribution to the total particle number and $PM_{0.15}$ mass concentration (mass of particles below 150 nm in diameter, converted from volume assuming sphericity) at the site. The method is not limited to particle number or volume concentration, but can also be used for different chemical species in both particle and gas phase. The total number of analyzed ship plumes was 726, covering on average 19 % of the time when air masses were arriving at the site over the shipping lane. During the periods when plumes were present, the particle concentration exceeded the background values on average by 790 cm^{-3} by number and 0.10 $\mu g\,m^{-3}$ by mass. The corresponding daily average values were 170 cm^{-3} and 0.023 $\mu g\,m^{-3}$, respectively. This means that the ship plumes contributed between 11 and 19 % to the particle number concentration and between 9 and 18 % to $PM_{0.15}$ during days when air was arriving over the shipping lane. The estimated annual contribution from ship plumes, where all wind directions were included, was in the range of 5–8 % in particle number concentration and 4–8 % in $PM_{0.15}$.

1 Introduction

Ship emissions and the subsequent chemical reactions in the ship plume lead to formation of ozone and particles, which have adverse health effects through inhalation and deposition in the human respiratory system. A health impact assessment points to a rate of 60 000 premature death cases annually and globally due to particle matter (PM) emitted by ships (Corbett et al., 2007). Ship emissions are also affecting the climate mainly through the emissions of nitrogen oxides (NO_x), sulfur dioxide (SO_2), carbon dioxide (CO_2) and

particles including black carbon (BC). The NO_x emissions mainly lead to a reduced methane lifetime over open ocean areas and hence result in a cooling effect (Bieltvedt Skeie et al., 2009). Emissions of SO_2 lead to the formation of sulfate aerosol particles, which generally have a cooling effect on the climate by direct scattering of solar radiation or indirectly, via the formation of cloud droplets (Bieltvedt Skeie et al., 2009). The combined effect of the greenhouse gas emissions and the climate cooling emissions from shipping is a net cooling of the climate at present conditions (Lauer et al., 2009; Bieltvedt Skeie et al., 2009; Fuglestvedt et al., 2009). New ship fuel sulfur regulations have been introduced limiting the ship fuel sulfur content to 0.5 % over open sea areas and to 0.1 % in selected emission control areas by 2020. The reduction of sulfur and NO_x emissions and accumulation of CO_2 due to ship emissions is likely to lead to a net warming due to ship emissions before the end of this century (Fuglestvedt et al., 2009). On the other hand, it also leads to a reduced premature mortality due to PM; Partanen et al. (2013) estimated a 96 % reduction in mortality due to ship emissions compared to the present day situation.

On ice-covered surfaces, there is one additional climatically important issue in ship emissions. When particulate BC deposits on snow- and ice-covered surfaces, the albedo of the surface decreases and melting is enhanced (Hansen and Nazarenko, 2004). Even though the ship-induced emissions of BC are minor compared to point source emissions of oil and gas exploitation, mining and other industrial sources (Ødemark et al., 2012), shipping is a diffuse source emitting BC over a much larger area (Berntsen et al., 2006). In addition to the warming effect of BC, the net radiation effect of SO_2 is also positive, though weak, in the Arctic since the anthropogenic emissions are leading to higher absorption of long-wave radiation by the relatively thin Arctic clouds (Garret and Zhao, 2006; Quinn et al., 2011; Mauritsen et al., 2011). Thus the total effect of shipping in the Arctic is probably a warming one. At present conditions, the warming effect is small, but it might become more important as the number of navigable shipping routes increases with a reduction of the Arctic sea ice area (Smith and Stephenson, 2013; Corbett et al., 2010).

To be able to estimate the global health and climate effects of ship-emitted particles in more detail, models require input data from measurements of the size-resolved emission factors of the particle number and mass concentration. In a global chemistry model, the fresh plumes emitted in a grid cell are diluted and aged before they are transported to the next grid cell on the order of 100 km away from the emission source. Hence, the fresh sub-grid emissions need to be transformed to aged emissions at the 100 km grid-scale level of such models. It is however, a challenge to parameterize this process in global models (Pierce et al., 2009). In addition, the parameterizations need to be validated against measurements of aged ship emissions.

Measurements of aged ship emissions are also necessary in order to study the contribution from ship emissions to the particle number and mass concentration downwind of a shipping lane, and to study the change in physical properties and chemical composition of particles due to ageing processes. Both of these factors are important and must be carefully considered in estimating health and climate predictions.

There are basically three approaches of how to experimentally determine emission factors of fresh and aged ship plumes in the atmosphere, and to evaluate how they contribute to downwind particle concentrations:

1. Measurements of individual ship plumes with an aircraft or ship vessel behind other ships can yield an estimate of the emission factors for both number and mass concentrations (Petzold et al., 2008; Lack et al., 2009).

2. Long-term on-shore measurements downwind of a shipping lane can yield the emission factors of ship plumes of an entire fleet of ships or alternatively individual ships with the help of ship position data (Jonsson et al., 2011). The contribution to particle number and mass concentrations at the shore line can also be estimated from such measurements.

3. Source/receptor modeling with chemical mass tracers downwind of shipping lanes or at harbors can be used to estimate the contribution to PM from shipping (Pandolfi et al., 2011).

Emission factors of particles in freshly emitted ship plumes have been estimated for individual and an ensemble of vessels using approach (2) in the study by Jonsson et al. (2011). The way fresh emissions are transformed during atmospheric ageing to plumes aged for several hours has been simulated by Tian et al. (2014). These authors have used aircraft data of fresh ship emissions of a few individual ships and an aerosol dynamics model to study the plume evolution. The modeled aged plumes were validated against measurements of roughly 1 hour old ship plumes from the data of many ships. The model showed that dilution reduced the number concentration by 4 orders of magnitude, and that coagulation reduced it by an additional order of magnitude after 1 hour. Although the general evolution is accounted for in a satisfactory way, the model yielded higher concentrations below 40 nm diameter compared to observations in the same study. One of the reasons for this finding might be that Tian et al. (2014) used a size distribution for the fresh plume which had a relatively high particle concentration in the sub-40 nm diameter range compared to for example the study by Jonsson et al. (2011).

In the current study, we have estimated how much ships do contribute to the on-shore particle number size distribution about 1 hour downwind of a major shipping lane in Denmark using long-term measurements (approach 2). Ship emissions in this area have previously been modeled based on Automatic Identification System (AIS) data (Olesen et al., 2009),

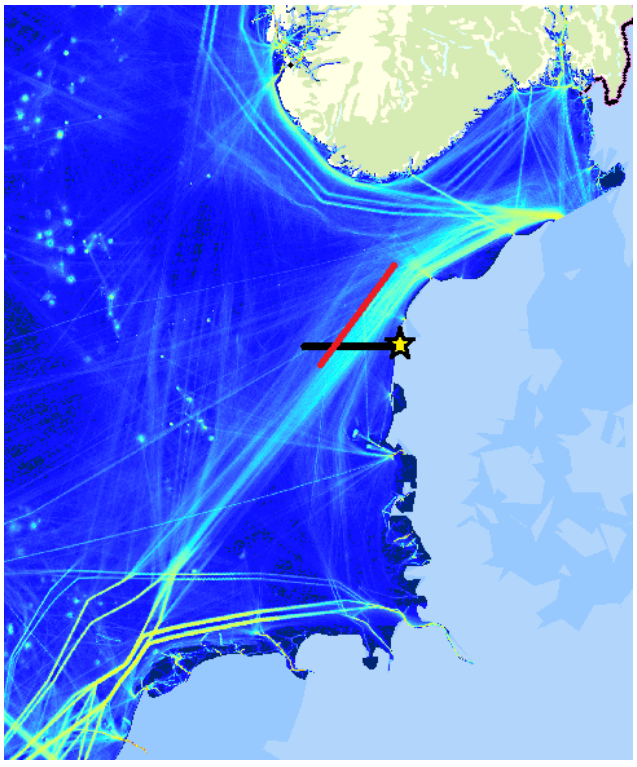

Figure 1. Map of total ship traffic in the western North Sea during the entire year 2012, based on the ship AIS data. The green and yellow lines show the shipping lanes where ships have operated during the year. The yellow and black star is the location of the Høvsøre measurement site. We used the red line for defining air mass trajectories arriving over the shipping lane (Sect. 2.1) and the black line for calculating the number of ships that pass the site (Sect. 2.2). Apart from the star and the red and black lines this figure is provided by the Norwegian Coastal Administration.

but no measurements were performed in their work. We have developed a new method to estimate this contribution, which is intended for use at other on-shore field sites. The method has been developed with the Arctic area in mind since ship emissions can have a large environmental and climate impact in this region. To the authors' knowledge this is the first study to address the contribution of one-hour aged ship plumes to the particle number size distribution measured on-shore based on the passage of several hundred ships. The method is suited to investigate how the particles are transformed about 1 hour downwind of the emission sources. The method is applicable to other emission species as well, and the results can be used for the parameterization of the plume transformation in global climate and air quality models.

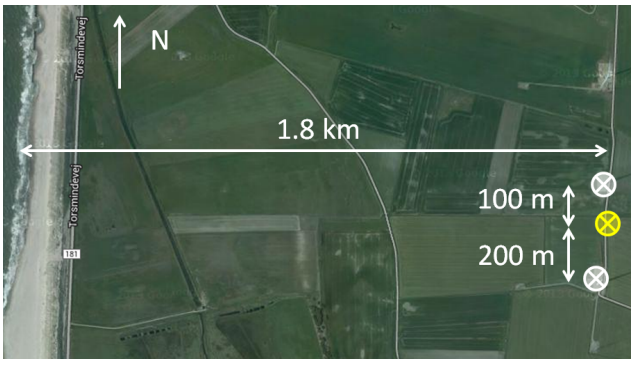

Figure 2. A close-up of the Høvsøre field site (yellow cross) with surrounding wind power turbines (white crosses). The sparsely trafficked local road (in north–south direction) is in the middle of the picture and the coastal road (Torsmindevej) is next to the coastline near the left edge of the picture.

2 Measurements and data

2.1 Høvsøre field site

Measurements were carried out at the wind power test facility station Høvsøre, Denmark (56°26′39″ N, 8°09′06″ E) (Fig. 1), between 9 March and 23 July 2012. The major offshore shipping lane northwest of the station is not defined by clear administratively set boundaries, as it is not in coastal waters. We have defined the shipping lane from AIS data showing where ships operate while passing the site. The distance from the station to the shipping lane is between 25 and 60 km depending whether the ships are on the closer or further edge of the shipping lane.

The measurement container hosting the instruments was positioned 1.8 km from the coastline (Fig. 2). The landscape between the coastline and the container is flat with very low elevation above sea level, except for a 5 m high and 10 m wide sand bank along the coastline. The container is surrounded by agricultural fields with very few trees, and 100 m to the NNW and 200 m to the SSW of the container, respectively, there are two wind turbines which spin occasionally but not continuously.

There is a road located about 1 km southwest of the container. Each day only a few cars pass by on this road. The local and tourism road along the coastline just to the east of the sand banks on the other hand, has a frequency of maximum 2500 vehicles per day during the summer. Zhang et al. (2004) showed that with an average traffic intensity of about 300 000 vehicles per day, measured particle number concentrations 300 m downwind of a major highway were not discernible from the upwind concentration. In their study the upwind concentration of particles between 6 and 220 nm in diameter was several thousand particles per cm^3 in the selected simulations. Based on this comparison, we argue that the coastline road near Høvsøre should have very minor or no impact

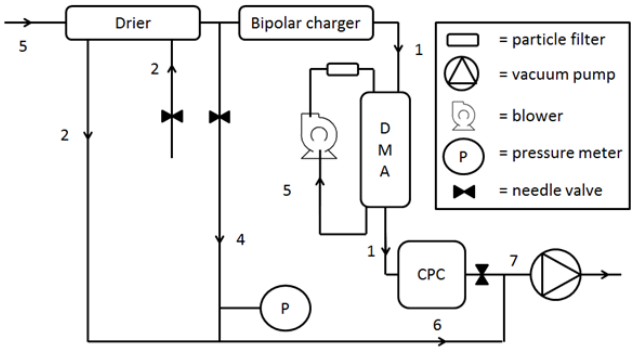

Figure 3. The drier and the SMPS configuration. Numbers are denoting flow rates in L min^{-1}.

on measured concentrations at the container, even though the background particle number concentrations are mostly lower. However, tractors at the fields, SUVs and maintenance vehicles servicing the wind turbines occasionally drove very close to the container. In such cases the particle number concentration was elevated in a narrow size range of the particle number size distribution, the effect lasting only a few tens of seconds.

2.2 Instrumentation

A scanning mobility particle sizer (SMPS) (TSI Inc., St. Paul, USA) was used to measure the particle number size distribution between 12.2 and 496 nm diameter (geometric mean diameters of the extreme bins) with 5 min time resolution. The instrument setup is shown in Fig. 3.

Before the aerosol particles entered the SMPS, they were dried with a Perma Pure fluorocarbon PD-070-18T-12 Nafion drier. A total aerosol volumetric flow of 5.0 L min^{-1} was let through the drier, which consisted of 18 internal drier tubing. A sheath flow of 2.0 L min^{-1} encompassed the tubing at about 180 mbar pressure to dry the particles in the aerosol flow. The drier was able to dry the particles in the aerosol flow to between 5 and 40 % relative humidity depending on the ambient conditions. The drier losses were slightly above 50 % at 12.2 nm diameter down to 0 % at 200 nm diameter. To take these losses into account, we divided the measured particle concentrations in each size bin by the size dependent fraction of particles that survived the drier.

Downstream of the drier, the flow was split into two parts, an aerosol flow of 1.0 L min^{-1} towards the SMPS and a 4.0 L min^{-1} bypass flow. The SMPS consisted of a bipolar Kr-85 charger, a differential mobility analyzer (DMA model 3080) and a TSI condensation particle counter (CPC model 3010). The DMA sheath flow was set to 5 L min^{-1}. The negative voltage of the DMA was continuously decreased for the first 240 s of the 5 min scan. During the subsequent 40 s, the voltage was continuously increased to the highest voltage. Then, a 20 s buffer time was used to let the instrument become stable before starting a new 5 min scan. Internal TSI software was used to invert the mobility distribution to a particle number size distribution taking into account the CPC efficiency, the tubing lengths, the residence time in the CPC and DMA, and multiple charging. The drier loss correction was applied after the inversion routine.

We quality controlled the data by looking at daily particle number size distribution plots. The short-term peaks caused by tractors and maintenance vehicles were identified for each size bin. If these peaks were more than 3 times higher than in the previous size bins during the DMA scanning, the entire 5 min size distribution was removed from the final data set. Also, periods when maintenance was performed on the SMPS system were removed from the data set. We did not find other instances when the data was faulty during quality control.

3 Methods

3.1 Trajectory analysis

We were interested in particles arriving from the shipping lane, which is located to the west and northwest of the station, but not in particles originating from other source areas. In order to separate the different sources we used Lagrangian Hybrid Single Particle Lagrangian Integrated Trajectory Model trajectories (Draxler and Hess, 1998). For each hour, we obtained 48 h backward trajectories arriving at Høvsøre at 100 m altitude. We checked that the trajectories were confined to the boundary layer for the last 5 hours before arriving at the measurement site. On average, the uncertainty of the trajectory path is 20 % of the trajectory length (Stohl et al., 1998), which in 50 km distance means 10 km in any horizontal direction.

We classified the trajectories into three trajectory types. Type 1 trajectories were those that had recently crossed the shipping lane before arriving at the site. This was defined such that the trajectory had to cross a line between 6°30′ E, 56°15′ N and 8°00′ E, 57°18′ N (representing the far edge of the shipping lane) within the previous 4 hours before arriving at Høvsøre (Figs. 1 and 4). Type 2 trajectories were those that arrived at Høvsøre from the sea, but did not fulfill the requirements to be classified as type 1. Type 3 trajectories arrived at the site from inland, even though many of them had been above sea earlier on their path.

We then classified days into five different categories based on the trajectories (Fig. 4). A ship day is a day when every trajectory during the 24 h was of type 1. A sea day is a day when every trajectory during the 24 h was of type 2. An inland day is a day when every trajectory during the 24 h was of type 3. If there were more than one type of trajectories during a day we classified it as a mixed day. Finally, we classified all days that had less than 10 available trajectories as missing data days.

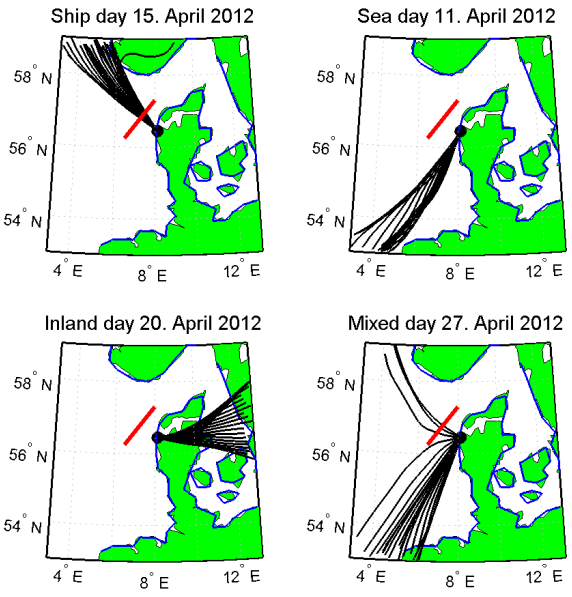

Figure 4. Maps of trajectories arriving at the Høvsøre site (marked with a black dot) during a ship day, a sea day, an inland day and a mixed day. The black lines represent all calculated air mass back trajectories during the day and the red line marks the section of the outer edge of shipping lane that the trajectories need to cross to be counted as having crossed the shipping lane.

We performed the trajectory analysis for all days during our measurement period (Table 1). In addition, we also carried out the same analysis for all days of the entire year 2012 in order to estimate the annual contribution.

3.2 Number of ships

The number of ships on the shipping lane passing by the Høvsøre site during each day was calculated using data from the ship Automatic Identification System, AIS (http://www.marinetraffic.com/; Winther et al., 2014). An AIS transponder is compulsory for all ships larger than 300 t in gross weight, except for military vessels. We only included in our calculation ships that had a registration number in the database of the International Maritime Organization, IMO, and that had an engine running. To estimate the number of ships passing by the measurement site we counted all ships that passed the 56°30′ N latitude parallel between longitudinal coordinates 6°30′ E and 8°12′ E (Fig. 1). The number of ships passing the site was calculated for each day of our measurement period. We separated the data into 1 day sections and counted the number of ships for each day. As the ship position in AIS system is given only every 6 min, we included all ship position data points between 56°24′ N and 56°36′ N in the data to make sure that we included all ships passing the site. This led to a situation where there was more than one data point per passing for some slower moving ships. In order to eliminate these multiple counts we allowed only one appearance per day for any individual ship.

3.3 Particle number size distribution during ship days

During ship days the particle number concentration was characterized by a smooth background level and sharp peaks clearly exceeding this level (Fig. 5). In the particle number size distribution data, these peaks were most dominant in the Aitken mode. During inland days no such peaks were present, but during other sea days there was sometimes some indication of more smoothed peaks. During mixed days there were clear peaks for some part of the day. Because we wanted to be sure that we were studying ship emissions, the analysis hereafter in this paper is applied only to ship days, unless mentioned otherwise. We have not made a direct connection between these peaks and the ships passing by, but since these peaks resemble ship plumes reported in other studies (Tian et al., 2014; Jonsson et al., 2011; Fridell et al., 2008; Isaksson et al., 2001) and there were no other plausible causes for the peaks, we assume that the peaks are produced by ship plumes. Later in this paper these peaks in the data are referred to as plumes.

3.4 Defining and extracting the ship plumes from the data

There were no measurements available of the same air masses prior to their crossing of the shipping lane. Therefore, we extracted the background particle number concentration and background particle number-size distribution from the total number concentration (N) and number-size distribution (PNSD) data that also contained the ship plumes. This was achieved by taking the 25th percentile values of a sliding window with a window width of 40 consecutive measurement points (3 h 20 min) of both N and PNSD (Fig. 5). In the following we call these data background particle number concentration (N_b) and background particle number size distribution ($PNSD_b$). We chose both the percentile and the window width by testing with different values. Higher percentile included plume values in N_b during periods of very frequent plumes, and a lower percentile followed the minimum points of N rather than the changes in the background level. The shorter time window also included plume values in N_b in case of long or frequent plumes.

We also calculated the particle volume concentration (V) and particle volume-size distribution (PVSD) by assuming that all particles are spherical and every particle has the geometric mean diameter of the corresponding size bin. Then we calculated the background particle volume concentration (V_b) and background particle volume-size distribution ($PVSD_b$) the same way as we did for the number concentrations number-size distribution. As most of the particle volume was located in the larger particle size range where the number concentration of particles was low and the counting

Table 1. Number and fraction of different types of days during our measurement period and during the entire year 2012.

Type of day	Number of days (measurement period)	Fraction of days (%, measurement period)	Fraction of days (%, entire year 2012)
Ship day	39	28.5	18.3
Sea day	17	12.4	10.9
Inland day	16	11.7	14.2
Mixed day	63	46.0	54.4
Missing data day	2	1.5	1.9
Total	137	100	99.9

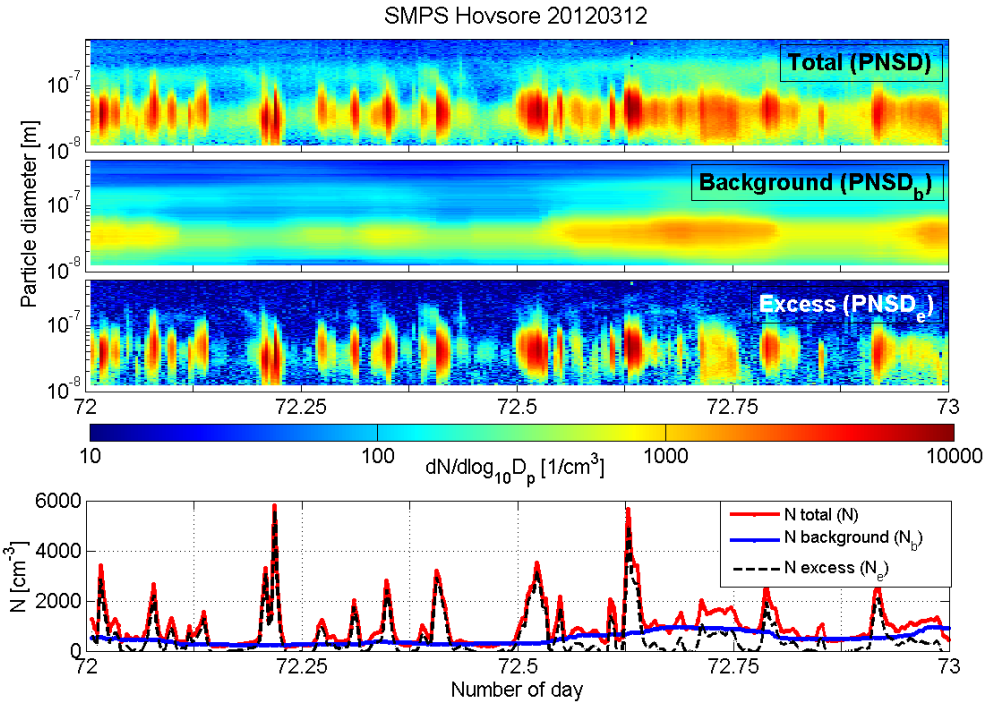

Figure 5. Three uppermost graphs: Color plots of total particle number size distribution (PNSD), background particle number size distribution ($PNSD_b$) and excess particle number size distribution ($PNSD_e$) as functions of time during 12 March 2012. All three graphs have the same color axis. Bottom graph: The corresponding number concentrations N, N_b and N_e as function of time.

statistics are thus poor, there was too much noise in V_b hiding any signal from the plume. To exclude the noisy data, we limited the particle volume analysis to 12–150 nm in diameter. We also analyzed the size range 12–300 nm, but in this size range the noise was already too high for reliable results. Therefore, we do not report numerical results for that size range.

We defined excess particle number concentration (N_e) and excess particle number-size distribution ($PNSD_e$) as the difference between the measured (total) N and PNSD, and the corresponding background values (N_b, $PNSD_b$) (Fig. 5). This data included the ship plumes as well as the noise in the measured data. In plotting, we replaced negative particle number concentrations in the N_e with 1 cm^{-3} and in V_e with 0.001 µm^3 cm^{-3}. The actual analysis, however, is done with data where the negative values were left intact. We defined the excess number ratio (R_{Ne}) and excess volume ratio (R_{Ve}) by dividing the measured total particle number (or volume) concentration by the background particle number (or volume) concentration.

If there were significant and rapid changes in the background particle number concentration (N_b), those could have affected our analysis later. We calculated the absolute and relative change rates of N_b and smoothed them by taking a sliding average of six consecutive measurement points (30 min). We marked any period when these smoothed values were above 56 cm^{-3} in absolute change or 5 % in relative change (or below −56 cm^{-3} or −5 %, respectively) as unanalyzable (Fig. 6). These values correspond to a change of 67 % of what is needed to define a plume (discussed later). We also

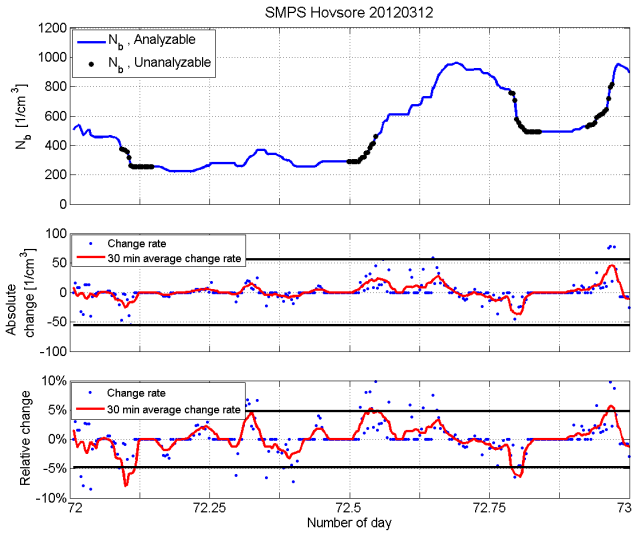

Figure 6. Uppermost graph: Background particle number concentration (N_b) as function of time during 12 March 2012 with analyzable and unanalyzable time periods marked separately. Middle graph: Absolute change rate of N_b from individual data points and as 30 min sliding average. The black lines are the threshold values for marking a time period unanalyzable ($\pm 56\,cm^{-3}$). Bottom graph: Same as middle graph but for relative change rate. Here the threshold values are $\pm 5\,\%$.

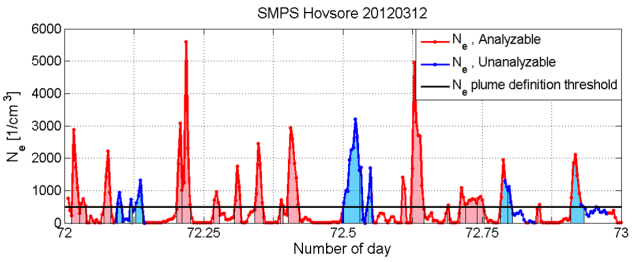

Figure 7. Number concentration of excess particles (N_e) as function of time during 12 March 2012. Unanalyzable time periods are marked with a blue line. Areas shaded with red are the analyzable plumes and areas shaded with blue are the unanalyzable plumes. Please note that even one unanalyzable data point makes the entire plume unanalyzable (e.g., the plume most to the right).

marked periods of 10 data points before any positive unanalyzable value and 10 data points after any negative unanalyzable value as unanalyzable, because due to the use of sliding 25th percentiles, the background reacted to decreasing concentrations roughly 10 measurement points too early and to increasing concentrations 10 measurement points too late. The unanalyzable periods covered 11 % of the total time during ship days, but when examined on daily basis the maximum unanalyzable period was 43 % of a day. All time periods that were not marked unanalyzable are considered analyzable. The analysis we present hereafter in this paper is done for analyzable periods only, unless mentioned otherwise.

We defined a plume as a period of data when $N_e >= 500\,cm^{-3}$ or $R_{Ne} >= 1.5$ (Fig. 7). These values are a compromise between including all clear plumes and excluding peaks caused by other variability in the data. If a continuous period defined by the above criteria contained several peaks in N_e or R_{Ne}, each peak was defined as a separate plume, separated by the time point with lowest N_e (or R_{Ne}) between the peaks. For each plume, we calculated the starting and the ending time of the plume, the plume duration, highest N_e in the plume, highest R_{Ne} in the plume and total N_e and V_e during the plume. If a plume contained even one data point within an unanalyzable period, the entire plume was marked as unanalyzable (Fig. 7). We also calculated the average particle number and volume size distributions of $PNSD_e$ and $PVSD_e$ for each plume, and fitted a lognormal curve to the average $PNSD_e$ of each plume. We converted the volume concentrations to mass concentrations ($PM_{0.15}$) assuming that all particles had a density of $1.5\,g\,cm^{-3}$, which is roughly in line with effective densities of aged soot particles measured in the area (Rissler et al., 2014).

Finally we calculated the total number of ship plumes per day, as well as daily average and sum values of the above parameters. We extrapolated the total daily number and volume concentrations of particles to cover also the unanalyzable periods of the day. This was done by dividing the daily values obtained from the analyzable time periods by the analyzable fraction of the day.

3.5 Calculating the ship plume contributions

We calculated the daily contribution of the ship plumes to total number N and total volume V with two different methods. The first method for calculating the contribution of ship plumes ($Ship N(\%)_{low}$) to daily particle number was done by dividing the sum of N_e values during all analyzable plumes (periods fulfilling the plume criteria) of that day with the sum of N values during all analyzable time periods of the same day according to Eq. (1):

$$Ship N(\%)_{low}(ship\,day) = \frac{\sum_{analyzable\,plumes} \sum_{plume\,start}^{plume\,end} N_e}{\sum_{analyzable\,time} N}. \quad (1)$$

The same procedure was done for the volume concentrations to obtain $Ship V(\%)_{low}(ship\,day)$. This method underestimates the plume contribution (and is therefore called $Ship N(\%)_{low}$ and $Ship V(\%)_{low}$) because it does not take into account those plumes where both N_e and R_{Ne} are below the plume definition limits we use or those parts of any plume that are below both of these limits. It also excludes in the numerator the analyzable part of any plume that has unanalyzable data, but includes that time period in the denominator.

The second method is given in Eq. (2):

$$\mathrm{Ship}N(\%)_{\mathrm{high}}\,(\mathrm{ship\,day}) = \frac{\sum_{\mathrm{analyzable\,time}} N_{\mathrm{e}}}{\sum_{\mathrm{analyzable\,time}} N}. \quad (2)$$

This method overestimates the plume contribution by including in the numerator not only all plumes, but also all noise in N_{e} and artificial peaks in N_{e} resulting from changes in N_{b} (those that are not high enough to be marked as unanalyzable). The same procedure was done for the volume concentrations to obtain Ship$V(\%)_{\mathrm{high}}$(ship day).

In order to estimate the average daily contribution of the ship plumes during ship days we calculated averages of the daily contributions for both methods separately, which gave us a range from the underestimating method value to the overestimating method value. We also calculated the lower estimate of ship plume contribution on N for a mixed day by Eq. (3):

$$\mathrm{Ship}N(\%)_{\mathrm{low}}\,(\mathrm{mixed\,day}) = \mathrm{Ship}N(\%)_{\mathrm{low}}\,(\mathrm{ship\,day})\,\frac{n\,(\mathrm{ship\,day})}{n\,(\mathrm{ship\,day}) + n\,(\mathrm{sea\,day}) + n\,(\mathrm{inland\,day})}, \quad (3)$$

where n denotes the number of each type of day during the entire year 2012. Then we performed the same calculation for Ship$N(\%)_{\mathrm{high}}$(mixed day) based on Ship$N(\%)_{\mathrm{high}}$(ship day) and the corresponding volume contributions using Ship$V(\%)_{\mathrm{low}}$(ship day) and Ship$V(\%)_{\mathrm{high}}$(ship day). Finally, we used these contributions to estimate the average contributions of ship plumes to N and V for the entire year 2012 based on the ship plume contributions for different types of days and the fraction of the different days during year 2012. In this analysis we assumed that there is no ship plume contribution during sea days or inland days and that a missing data day gives the same contribution as a mixed day.

$$\mathrm{Ship}N\,(\%)_{\mathrm{low}}\,(2012) = \frac{n\,(\mathrm{ship\,day}) \times \mathrm{Ship}N(\%)_{\mathrm{low}}\,(\mathrm{ship\,day}) + (n\,(\mathrm{mixed\,day}) + n\,(\mathrm{missing\,data\,day})) * \mathrm{Ship}N(\%)_{\mathrm{low}}\,(\mathrm{mixed\,day})}{n\,(\mathrm{ship\,day}) + n\,(\mathrm{sea\,day}) + n\,(\mathrm{inland\,day}) + n\,(\mathrm{mixed\,day}) + n\,(\mathrm{missing\,data\,day})} \quad (4)$$

We calculated the overestimation values for the entire year 2012 the same way from the Ship$N(\%)_{\mathrm{high}}$ values, and the volume contributions from Ship$V(\%)_{\mathrm{low}}$ and Ship$V(\%)_{\mathrm{high}}$ values.

4 Results

4.1 Number of ships

The daily number of ships passing the Høvsøre site was, on average, 82 ships per day, and varied from 64 to 97 ships per day (10 and 90 percentiles) during our measurement period. On average 40 (32 to 48) of them were ships registered with size larger than 10 kt in gross weight. We can assume that these large ships produce the strongest plumes, having highest probability for detection. Therefore, we can expect the daily number of detectable plumes to be around those numbers. If an individual ship passed the site twice the same day, it was counted only once, which can lead to a slight underestimation of these numbers. This underestimation is assumed to affect mostly the number of smaller vessels that operate around the area rather than pass by on the shipping lane. A significant amount of activity of smaller ships took place at the nearby small harbors of Thyborøn and Thorsminde 28 km north and 8 km south of the Høvsøre measurement site, respectively. We do not expect any contribution from ships at those areas in our measurements, since a trajectory arriving over the locations of the harbors would most likely not be classified as having arrived from the shipping lane (see Sect. 3.1), and therefore the day would not be classified as a ship day and thus analyzed. All activities of ships larger than 10 kt in gross weight were on the open sea, mostly in the shipping lane.

4.2 Characteristics of the ship plumes

There were altogether 726 analyzable ship plumes detected during ship days in our measurement data. Of the plumes, 355 (49%) were separate plumes with N_{e} exceeding 500 cm^{-3} and 156 (21 %) were separate plumes with N_{e} <500 cm^{-3} but $R_{\mathrm{Ne}} > 1.5$. The remaining 215 (30 %) plume peaks were peaks not separated by non-plume periods.

The average duration of a plume was 12 min. (Table 2). The duration varied from 5 to 25 min (10 and 90 % values). It is worth noticing that 36 % of the plumes had the minimum duration of one measurement cycle lasting 5 min.

Table 2 summarizes the plume characteristics with average values as well as 10 and 90 percentiles. We calculated the peak height of the number concentration of excess particles (N_{e} peak). The start and end times of the plumes allowed us to calculate the average N_{e} during each individual plume (N_{e} plume average). We also calculated the sum of N_{e} for the entire day, and then divided it over the analyzable periods of the day (N_{e} day average).

We also report the corresponding values for V_{e}, converted into $PM_{0.15}$ (Table 2). These values are very low when compared to typically reported PM_1 and $PM_{2.5}$ contributions from shipping using source/receptor modeling (Pandolfi et al., 2011, and references therein). However, one should keep in mind that our values are only for very small particles $PM_{0.15}$ whereas most of PM_1 or $PM_{2.5}$ mass is contributed by the larger particles. In some plumes we observed another particle mode with a diameter around 200 nm. This mode did not contribute much to N_{e}, while the volume concentration of particles in this mode (even though often significant) was usually masked by the high noise in the calculated total volume concentration (V).

The average particle number size distribution of excess particles ($PNSD_{\mathrm{e}}$) during plumes peaked at 41 nm whereas $PVSD_{\mathrm{e}}$ peaked at 76 nm (Fig. 8). Some of the individual

Table 2. Characteristic values of the plumes. Calculation of N_e peak, plume average and day average. The average fitted number concentration N, geometric standard deviation σ and mode peak diameter D_p (with 10 and 90 % values) of N_e.

Parameter	Unit	10 % value	Average value	90 % value
Plume duration	min	5	12	25
N_e peak	cm^{-3}	170	970	2200
N_e plume average	cm^{-3}	140	790	1700
N_e day average	cm^{-3}	16	170	420
$PM_{0.15}$ plume average	$\mu g\,m^{-3}$	0.014	0.10	0.24
$PM_{0.15}$ day average	$\mu g\,m^{-3}$	0.0017	0.023	0.057
Fitted N plume average	cm^{-3}	190	830	1900
Fitted σ plume average	–	1.34	1.52	1.88
Fitted D_p plume average	nm	20	39	52

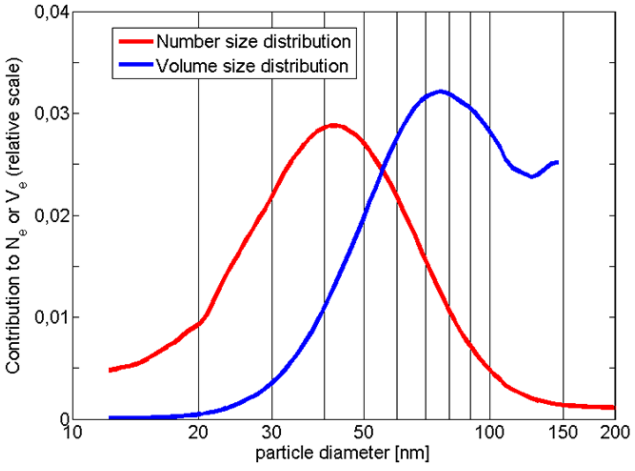

Figure 8. Average particle size distributions of excess particles by number ($PNSD_e$) and volume ($PVSD_e$) between 10 and 200 nm in diameter.

$PVSD_e$ had highest values at 150 nm. This can be caused by the 200 nm mode or by the noise, as described above. The average fitted number concentration N, geometric standard deviation σ and mode peak diameter D_p (with 10 and 90 % values) of N_e are also presented in Table 2.

The number of valid ship plumes per day was on average 19 and varied from 5 to 32 plumes (10 and 90 percentiles) per day (Table 3). We also extrapolated these values to cover the unanalyzable periods and calculated the total duration of all analyzable plumes during the day as well as their fraction of the total analyzable time of the day. There was no single day where the number of observed ship plumes exceeded the number of ships larger than 10 kt in gross weight.

4.3 Contribution of the ship plumes to particle number and volume

We calculated the average daily ship plume contributions to N_e and V_e at Høvsøre (Table 4) as described in the methods section. The lower limits of the ranges are mean values calculated with the underestimating method ($Ship N(\%)_{low}$ and $Ship V(\%)_{low}$), and the higher limits are mean values calculated with the overestimating method ($Ship N(\%)_{high}$ and $Ship V(\%)_{high}$). The estimates for the entire year are based on the average daily contributions and the fraction of different days during the year.

5 Discussion

The use of sliding percentile as a filter for extracting peak values from background values is, in the field of statistics, not a new idea (e.g., Torrence and Compo, 1998), but we are not aware of it being used for extracting ship plumes from background data before this paper. Similar methods are used in other applications but for data where the peaks have already been removed (e.g., European Commission, 2011; Escudero et al., 2007). The use of a sliding median or percentile (instead of sliding average) means that peak values do not directly affect the background level. There are, however, some biases produced by the method. In our case the use of a percentile lower than 50 % means that even during periods when there are no peaks within the sliding window (40 consecutive data points) more than half of the noise is included in N_e and less than half in N_b, and therefore the extracted N_b is somewhat lower than the average of the window. Peaks within the sliding window increase N_b (and decrease N_e) slightly by replacing some of the low values within the window with high ones, therefore increasing the 25 % value. If the noise in N is much smaller than the peak values, neither one these biases has a significantly effect on the analysis. When we use the

Table 3. Daily values of the plume parameters. Some of the values are extrapolated to also cover the unanalyzable time periods of the day.

Parameter	Unit	10 % value	Average value	90 % value
Analyzable time	% of day	75	89	100
Plumes	–	6	24	37
Analyzable plumes	–	5	19	32
Analyzable plumes, extrapolated	–	5	21	35
Plume time	min	74	210	430
Plume time, extrapolated	min	74	270	520
Plume time, extrapolated	% of day	5	19	30

Table 4. Ship plume contribution to number and volume of particles at Høvsøre during a ship day, a mixed or missing data day and for the entire year 2012.

	Ship plume contribution during average ship day (%)	Ship plume contribution during average mixed or missing data day (%)	Ship plume contribution during entire year 2012 (%)
Number	11–19	5–8	5–8
$PM_{0.15}$	9–18	4–8	4–8

25th percentile, actual peak values are included in N_b only if the peak periods cover more than 75 % of the given time window.

We found the ship plumes contribute daily, on average, between 11 and 19 % to the total number concentration and between 9 and 18 % to $PM_{0.15}$ at Høvsøre on the western coast of Denmark during days when the wind was blowing from the shipping lane. When this was extrapolated to the entire year 2012 taking into account the fraction of different types of days, the corresponding numbers were between 5 and 8 % for total particle number concentration and between 4 and 8 % for $PM_{0.15}$. This extrapolation does not take into account any systematic seasonal differences in background particle number concentration, background particle number-size distribution or in shipping intensity, and is therefore to be used only as a rough estimate.

Even though we have reported an upper and lower limit for our estimates, the whole range could be somewhat too low. We have included plumes only from the nearby shipping lane whereas plumes from ships further away are more diluted and contribute as an increase in the background particle number and volume concentrations, therefore decreasing the calculated contributions in our approach instead of increasing them. The same applies to the most diluted plumes from the nearby shipping lane. In general, the method tends to underestimate the number of individual plumes while aged, non-detected plumes can increase the background concentrations. Furthermore, we have assumed the sea days (air coming from the sea, but not perpendicularly over the nearby shipping lane) to have a ship plume contribution of zero. There are cases when, during a sea day, air parcels pass along the shipping lane for some time of the day, and these also transport ship-emitted particles to our measurement site.

The mass contribution of $PM_{0.15}$ we obtain in this study is only 1 to 10 % of the $PM_{2.5}$ contribution reported at other shore or port areas (Pandolfi et al., 2011, and references therein) at similar or shorter distances to the ships. Despite the fact that most of the particles are found in the sub-150 nm diameter size range, the $PM_{2.5}$ contribution is often dominated by a few, but rather large particles. Also, the lower emission limits in the Baltic and North seas (IMO, 2008) can decrease the particle mass concentrations observed in this study.

The plumes observed in this study had an average peak diameter of 41 nm (39 nm in the fitted mode). This is generally larger than what has been reported for fresh ship plumes under laboratory conditions (Kasper et al., 2007; Petzold et al., 2008), onboard a ship (Fridell et al., 2008) or onshore in harbor areas (Jonsson et al., 2011; Isakson et al., 2001). However, for some engine loads the difference between other reported peak diameters and the one reported in this study is negligible (Petzold et al., 2008). The size difference indicates that the particles in the plumes grow in size during the first hours after being emitted. This transformation is proposed to be used for validating the parameterized transformation of ship plumes in global models. We also observed another mode with a peak diameter between 100 and 200 nm in many plumes, but our data was not sufficient for analyzing that mode properly. This mode has been reported in several other studies, and is assumed to consist of mainly soot,

organic carbon and sulfates (Lieke et al., 2013; Popovicheva et al., 2012; Moldanova et al., 2009).

Based on the number of ships, it is clear that we are not able to distinguish the plumes of all ships in the area, even during periods of favorable wind directions. When air arrived over the shipping lane (ship days), the daily total number of plumes (including the unanalyzable ones) was only 30 % of the total number of ships, and 59 % of the total number of ships above 10 kt in gross weight. When only analyzable plumes were taken into account, but their number was extrapolated to account for the unanalyzable periods, the corresponding numbers became 27 and 53 %, respectively.

There are at least three possible reasons why we were not able to distinguish and detect plumes from all individual ships:

Probably the most important reason for this finding is the fact that a large fraction of the ships are small, and therefore do not produce strong enough individual plumes to be detected by our method after some aging. If the number of these plumes is not very high, they will be included in the upper estimates of the ship contribution. If these plumes cover a high enough time fraction of a given time period, they will contribute to the background level and, as discussed above for ship emissions further away, therefore decrease both estimates of the plume contribution.

Another reason is the different distances between the ships and our measurement site. If a ship passes further away the plume has more time to dilute and disperse, and thus could not be recognized as a plume by our method, but it would be included in the upper estimates of the ship contribution. If a plume is extremely dispersed, it can even contribute to background values.

The third reason lies in the uncertainties created by the meteorological conditions, especially the boundary layer height. A higher well-mixed boundary layer allows more vertical mixing of the plume leading to lower particle number and volume concentrations at our measurement site. Also, enhanced deposition (e.g., rain) can lower the particle number concentration significantly. These factors affect not only the plume, but also the background concentrations, and therefore many (but not all) of these plumes are included in the analysis as plumes with $N_e < 500\,cm^{-3}$ but $R_{Ne} >= 1.5$.

6 General conclusions

In general, we can claim that this method works in areas where ship traffic is emitting particles to an otherwise homogenous particle population. The less variation there is in the background number and volume concentrations, the better the developed method works. Also, fewer ships would make it easier to separate the individual plumes, as one can use sliding median instead of sliding 25th percentile as a background filter. This would decrease the duration of unanalyzable periods. Suitable places for applying this analysis can be found, for example, in the Arctic and at oceanic coasts where the prevailing winds are marine. In places where the orography is complex, the boundary layer may create local effects that disturb the air flow, and therefore we do not recommend using this technique at mountainous shores without further examination.

In the near future it is important to parameterize the effects of meteorology on observed plumes in order to make the different days of observation more comparable. If the plumes arrive at the measurement site in less than 45 min, independent high time resolution measurements of CO_2, NO_x and SO_2 could validate the occurrence of the plumes better (Petzold et al., 2008). Higher time resolution particle number concentration measurements could contribute with valuable additional information. Finally, measurements of particle mass or mass-size distribution with high enough time resolution would allow much better analysis of the ship contribution to PM_1 or $PM_{2.5}$. Combining trajectory and ship AIS information will make it possible to connect the plumes to individual ships, and therefore to evaluate in detail how individual ships contribute to the particle population.

Acknowledgements. This work was supported by NordForsk through the top-level initiative Cryosphere-atmosphere interactions in changing Arctic climate (CRAICC) and the Swedish research council FORMAS (grant no. 2010–850). The study is a contribution to the Lund University Strategic Research Areas: Modeling the Regional and Global Earth System (MERGE). The Nordea Foundation is acknowledged for financial support of the measurement container. We also thank Norwegian Coastal Authority for providing us the AIS data.

Edited by: S. M. Noe

References

Berntsen, T., Fuglestvedt, J., Myhre, G., Stordal, F., and Berglen, T.: Abatement of greenhouse gases: Does location matter?, Clim. Change, 74, 377–411, doi:10.1007/s10584-006-0433-4, 2006.

Bieltvedt Skeie, R., Fuglestvedt, J., Berntsen, T., Tronstad Lund, M., Myhre, G., and Rypdahl, K.: Global temperature change from the transport sectors: Historical development and future scenarios, Atmos. Environ., 43, 6260–6270, 2009.

Corbett, J. J., Winebrake, J. J., Green, E. H., Kasibhatla, P., Eyring, V., and Lauer, A.: Mortality from ship emission: A global assessment, Environ. Sci. Technol., 41, 8512—8518, 2007.

Corbett, J. J., Lack, D. A., Winebrake, J. J., Harder, S., Silberman, J. A., and Gold, M.: Arctic shipping emissions inventories and future scenarios, Atmos. Chem. Phys., 10, 9689–9704, doi:10.5194/acp-10-9689-2010, 2010.

Draxler, R. R. and Hess, G. D.: An overview of the HYSPLIT_4 modeling system of trajectories, dispersion, and deposition, Aust. Meteorol. Mag., 47, 295–308, 1998.

Escudero, M., Querol, X., Pey, J., Alastuey, A., Pérez, N., Ferreira, F., Alonso, S., Rodríquez, S., and Cuevas, E.: A methodology for the quantification of the net African dust load in air quality

monitoring networks. Guidance to Member States on PM_{10} monitoring and intercomparisons with the reference methods, Atmos. Environ. 41, 5516–5524, 2007.

European Comission: Commission Staff Working Paper: establishing guidelines for demonstration and subtraction of exceedances attributable to natural sources under Directive 2008/50EC on ambient air quality and cleaner air for Europe, SEC(2011) 208 final, available at http://ec.europa.eu/environment/air/quality/legislation/pdf/sec_2011_0208.pdf (last access: 18 March 2014), 2011

Fridell, E., Steen, E., and Peterson, K.: Primary particles in ship emissions, Atmos. Environ., 42, 1160–1168, 2008.

Fuglestvedt, J., Berntsen, T., Eyring, V., Isaksen, I., Lee, D. S., and Sausen, R.: Shipping Emissions: From Cooling to Warming of Climate – And Reducing Impacts on Health, Environ. Sci. Technol., 43, 5592–5598, 2009.

Garrett, T. J. and Zhao, C.: Increased Arctic cloud longwave emissivity associated with pollution from mid-latitudes, Nature, 440, 787–789, doi:10.1038/nature04636, 2006.

Hansen, J. and Nazarenko, L.: Soot climate forcing via snow and ice albedos, P. Natl. Acad. Sci. USA, 101, 423–428, 2004.

IMO (International Maritime Organization), Amendments to the annex of the protocol of 1997 to amend the international convention for the prevention of pollution from ships, 1973, as modified by the protocol of 1978 relating thereto, available at: http://www.imo.org/OurWork/Environment/PollutionPrevention/AirPollution/Documents/Air%20pollution/Resolution%20MEPC.176(58)%20Revised%20MARPOL%20Annex%20VI.pdf (last access: 6 March 2014), 2008.

Isakson, J., Persson, T. A., and Selin Lindgren, E.: Identification and assessment of ship emissions and their effects in the harbor of Göteborg, Sweden, Atmos. Environ., 35, 3659–3666, 2001.

Jonsson, Å. M., Westerlund, J., and Hallquist, M.: Size-resolved particle emission factors for individual ships, Geophys. Res. Lett., 38, L13809, doi:10.1029/2011GL047672, 2011.

Kasper, A., Aufdenblatten, S., Forss, A., Mohr, M., and Burtscher, H.: Particulate emissions from a low-speed marine diesel engine, Aerosol Sci. Tech., 41, 24–32, 2007.

Lack, D., Corbett, J. J., Onasch, T., Lerner, B., Massoli, P., Quinn, P. K., Bates, T., Covert, D., Coffman, D., Sierau, B., Herndon, S., Allan, J., Baynard, T., Lovejoy, E., Ravishankara, A. R., and Williams, E.: Particulate emissions from commercial shipping: Chemical, physical, and optical properties, J. Geophys. Res., 114, D00F04, doi:10.1029/2008JD011300, 2009.

Lauer, A., Eyring, V., Corbett, J. J., Wang, C., and Winebrake, J. J.: Assessment of Near-Future Policy Instruments for Oceangoing Shipping: Impact on Atmospheric Aerosol Burdens and the Earth's Radiation Budget, Environ. Sci. Technol., 43, 5592–5598, 2009.

Lieke, K. I., Rosenørn, T., Pedersen, J., Larsson, D., Kling, J., Fuglsang, K., and Bilde, M.: Micro- and Nanostructural Characteristics of Particles Before and After an Exhaust Gas Recirculation System Scrubber, Aerosol Sci. Tech., 47, 1038–1046, doi:10.1080/02786826.2013.813012, 2013.

Mauritsen, T., Sedlar, J., Tjernström, M., Leck, C., Martin, M., Shupe, M., Sjogren, S., Sierau, B., Persson, P. O. G., Brooks, I. M., and Swietlicki, E.: An Arctic CCN-limited cloud-aerosol regime, Atmos. Chem. Phys., 11, 165–173, doi:10.5194/acp-11-165-2011, 2011.

Moldanova, J., Fridell, E., Popovicheva, O., Demirdjian, B., Tishkova, V., Faccinetto, A., and Focsa, C.: Characterization of particulate matter and gaseous emissions from a large ship diesel engine, Atmos. Environ., 43, 2632–2641, 2009.

Ødemark, K., Dalsøren, S. B., Samset, B. H., Berntsen, T. K., Fuglestvedt, J. S., and Myhre, G.: Short-lived climate forcers from current shipping and petroleum activities in the Arctic, Atmos. Chem. Phys., 12, 1979–1993, doi:10.5194/acp-12-1979-2012, 2012.

Olesen, H. R., Winther, M., Ellermann, T., Christensen, S. and Plejdrup, M.: Ship emissions and air pollution in Denmark – Present situation and future scenarios, National Environmental Research Institute, Aarhus University, Aarhus, Denmark, Environmental Project No. 1307, 134 pp., 2009.

Pandolfi, M., Gonzales-Castanedo, Y., Alastyey, A., de la Rosa, J. D., Mantilla, E., de la Campa, S. S., Querol, X., Pey, J., Amato, F., and Moreno, T.: Source apportionment of PM_{10} and $PM_{2.5}$ at multiple sites in the strait of Gibraltar by PMF: impact of shipping emissions, Environ. Sci. Pollut. R., 18, 260–269, doi:10.1007/s11356-010-0373-4, 2011.

Partanen, A. I., Laakso, A., Schmidt, A., Kokkola, H., Kuokkanen, T., Pietikäinen, J.-P., Kerminen, V.-M., Lehtinen, K. E. J., Laakso, L., and Korhonen, H.: Climate and air quality tradeoffs in altering ship fuel sulfur content, Atmos. Chem. Phys., 13, 12059–12071, doi:10.5194/acp-13-12059-2013, 2013.

Petzold, A., Hasselbach, J., Lauer, P., Baumann, R., Franke, K., Gurk, C., Schlager, H., and Weingartner, E.: Experimental studies on particle emissions from cruising ship, their characteristic properties, transformation and atmospheric lifetime in the marine boundary layer, Atmos. Chem. Phys., 8, 2387–2403, doi:10.5194/acp-8-2387-2008, 2008.

Pierce, J. R., Theodoritsi, G., Adams, P. J., and Spandis, S. N.: Parameterization of the effect of sub-grid scale aerosol dynamics on aerosol number emission rates, J. Aerosol Sci., 40, 385–393, 2009.

Popovicheva, O., Kireeva, E., Persiantseva, N., Timofeev, M., Bladt, H., Ivleva, N. P., Niessner, R., and Moldanova, J.: Microscopic characterization of individual particles from multicomponent ship exhaust, J. Environ. Monitor., 14, 3101, doi:10.1039/c2em30338h, 2012.

Quinn, P. K., Stohl, A., Arneth, A., Berntsen, T., Burkhart, J. F., Christensen, J., Flanner, M., Kupiainen, K., Lihavainen, M., Shepherd, M., Shevchenko, V., Skov, H., and Vestreng, V.: AMAP 2011, The Impact of Black Carbon on Arctic Climate. Arctic Monitoring and Assessment Programme (AMAP), Oslo, 72 pp., 2011.

Rissler, J., Nordin, E. Z., Eriksson, A. C., Nilsson, P. T., Frosch, M., Sporre, M. K., Wierzbicka, A., Svenningsson, B., Löndahl, J., Messing, M. E., Sjogren, S., Hemmingsen, J. G., Loft, S., Pagels, J. H., and Swietlicki, E.: Effective Density and Mixing State of Aerosol Particles in a Near-Traffic Urban Environment, Environ. Sci. Technol., 48, 6300–6308, doi:10.1021/es5000353, 2014.

Smith, L. and Stephenson, S.: New Trans-Arctic shipping routes navigable by midcentury, P. Natl. Acad. Sci., 110, E1191–E1195, doi:10.1073/pnas.1214212110, 2013.

Stohl, A.: Computation, Accuracy, and applications of trajectories – a review and bibliography, Atmos. Environ., 32, 947–966, 1998.

Tian, J., Riemer, N., West, M., Pfaffenberger, L., Schlager, H., and Petzold, A.: Modeling the evolution of aerosol particles in a ship

plume using PartMC-MOSAIC, Atmos. Chem. Phys., 14, 5327–5347, doi:10.5194/acp-14-5327-2014, 2014.

Torrence, C. and Compo, G. P.: A Practical Guide to Wavelet Analysis, B. Am. Meteorol. Soc., 79, 61–78, 1998.

Winther, M., Christensen, J. H., Plejdrup, M. S., Ravn, E. S., Eriksson, Ó. F., and Kristensen, H. O.: Emission inventories for ships in the Arctic based on AIS data, Atmos. Environ., 91, 1–14, 2014.

Zhang, K. M., Wexler, A. S., Zhu, Y. F., Hinds, W. C., and Sioutas, C.: Evolution of particle number distribution near roadways. Part II: the "Road-To-Ambient" process, Atmos. Environ., 38, 6655–6665, 2004.